CHANGE DETECTION IN A SHORT TIME SEQUENCE OF POLARIMETRIC C-BAND SAR DATA

Allan Aasbjerg Nielsen[(1)], Knut Conradsen[(1)], and Henning Skriver[(2)]

[(1)]*DTU Compute – Applied Mathematics and Computer Science, {alan,knco}@dtu.dk*
[(2)]*DTU Space – National Space Institute, hs@space.dtu.dk*
Technical University of Denmark
DK-2800 Kgs. Lyngby, Denmark

ABSTRACT

Based on an omnibus likelihood ratio test statistic for the equality of several variance-covariance matrices following the complex Wishart distribution and a factorization of this test statistic with associated p-values, change analysis in a time series of multilook, polarimetric SAR data in the covariance matrix representation is carried out. The omnibus test statistic and its factorization detect if and when change(s) occur. The technique is demonstrated on airborne EMISAR C-band data but may be applied to ALOS, COSMO-SkyMed, RadarSat-2 Sentinel-1, TerraSAR-X, and Yaogan data also.

1. INTRODUCTION

In earlier publications we have described a test statistic for the equality of two variance-covariance matrices following the complex Wishart distribution with an associated p-value [1]. We showed their application to bitemporal change detection and to edge detection [2] in multilook, polarimetric synthetic aperture radar (SAR) data in the covariance matrix representation. The test statistic and the associated p-value is described in [3] also. In [4] we focused on the block-diagonal case, we elaborated on some computer implementation issues, and we gave examples on the application to change detection in both full and dual polarization bitemporal, bifrequency, multilook SAR data.

In [5] we described an omnibus test statistic Q for the equality of $k \geq 2$ variance-covariance matrices following the complex Wishart distribution. We also described a factorization of $Q = \prod_{j=2}^{k} R_j$ where Q and R_j determine if and when a difference occurs. Additionally, we gave p-values for Q and R_j. Finally, we demonstrated the use of Q and R_j and the p-values to change detection in truly multitemporal, full polarization SAR data. For more references to change detection in polarimetric SAR data, see [5].

In [5] we applied the methods to a series of EMISAR [6,7] L-band data. In this paper we apply the methods to EMISAR C-band data. The methods may be applied to other polarimetric SAR data also such as data from ALOS, COSMO-SkyMed, RadarSat-2 Sentinel-1, TerraSAR-X, and Yaogan.

2. TEST STATISTICS AND THEIR DISTRIBUTIONS

This section gives the main results from [5]. The average covariance matrix for multilook polarimetric SAR is defined as [8]

$$\langle \boldsymbol{C} \rangle = \begin{bmatrix} \langle S_{hh}S_{hh}^* \rangle & \langle S_{hh}S_{hv}^* \rangle & \langle S_{hh}S_{vv}^* \rangle \\ \langle S_{hv}S_{hh}^* \rangle & \langle S_{hv}S_{hv}^* \rangle & \langle S_{hv}S_{vv}^* \rangle \\ \langle S_{vv}S_{hh}^* \rangle & \langle S_{vv}S_{hv}^* \rangle & \langle S_{vv}S_{vv}^* \rangle \end{bmatrix} \quad (1)$$

where $\langle \cdot \rangle$ denotes ensemble averaging and * denotes complex conjugation. S_{rt} denotes the complex scattering amplitude for receive and transmit polarization ($r, t \in \{h, v\}$ for horizontal and vertical polarization).

2.1. Test for equality of several complex covariance matrices

To test whether a series of $k \geq 2$ complex variance-covariance matrices $\boldsymbol{\Sigma}_i$ are equal, i.e., to test the null hypothesis H_0

$$H_0 : \boldsymbol{\Sigma}_1 = \boldsymbol{\Sigma}_2 = \cdots = \boldsymbol{\Sigma}_k$$

against all alternatives, we use the following omnibus test statistic (for the real case see [9]; for the case with two complex matrices see [1, 2]; $|\cdot|$ denotes the determinant)

$$Q = \left\{ k^{pk} \frac{\prod_{i=1}^{k} |\boldsymbol{X}_i|}{|\boldsymbol{X}|^k} \right\}^n . \quad (2)$$

Here the $\boldsymbol{\Sigma}_i$ (and the $\boldsymbol{X}_i$) are p by p ($p = 3$ for full pol data, $p = 2$ for dual pol data, and $p = 1$ for single channel power data), and the $\boldsymbol{X}_i = n\hat{\boldsymbol{\Sigma}}_i = n\langle \boldsymbol{C} \rangle_i$ follow the complex Wishart distribution, i.e., $\boldsymbol{X}_i \sim W_C(p, n, \boldsymbol{\Sigma}_i)$. Further, $\boldsymbol{X} = \sum_{i=1}^{k} \boldsymbol{X}_i \sim W_C(p, nk, \boldsymbol{\Sigma})$. If the hypothesis is true ("under

Proc. 'Living Planet Symposium 2016', Prague, Czech Republic, 9–13 May 2016 (ESA SP-740, August 2016)

Table 1. Part of the change analysis structure for an example with data from four time points.

	$t_1 = \cdots = t_4$	$t_2 = \cdots = t_4$	$t_3 = t_4$
Omnibus	$Q^{(1)}$: $P\{Q^{(1)} < q^{(1)}_{\rm obs}\}$	$Q^{(2)}$: $P\{Q^{(2)} < q^{(2)}_{\rm obs}\}$	$Q^{(3)}$: $P\{Q^{(3)} < q^{(3)}_{\rm obs}\}$
$t_1 = t_2$	$R^{(1)}_2$: $P\{R^{(1)}_2 < z^{(1)}_{2,\rm obs}\}$		
$t_2 = t_3$	$R^{(1)}_3$: $P\{R^{(1)}_3 < z^{(1)}_{3,\rm obs}\}$	$R^{(2)}_2$: $P\{R^{(2)}_2 < z^{(2)}_{2,\rm obs}\}$	
$t_3 = t_4$	$R^{(1)}_4$: $P\{R^{(1)}_4 < z^{(1)}_{4,\rm obs}\}$	$R^{(2)}_3$: $P\{R^{(2)}_3 < z^{(2)}_{3,\rm obs}\}$	$R^{(3)}_2$: $P\{R^{(3)}_2 < z^{(3)}_{2,\rm obs}\}$

Table 2. Average no-change probabilities for the grass field.

	$t_1 = \cdots = t_4$	$t_2 = \cdots = t_4$	$t_3 = t_4$
Omnibus	0.0049	0.0076	0.1213
$t_1 = t_2$	0.2883		
$t_2 = t_3$	0.1372	0.1500	
$t_3 = t_4$	0.0248	0.0378	0.1213

H_0" in statistical parlance), $\hat{\mathbf{\Sigma}} = \boldsymbol{X}/(kn)$. $Q \in [0,1]$ with $Q = 1$ for equality.

For the logarithm of the test statistic we get

$$\ln Q \;=\; n\left\{pk\ln k + \sum_{i=1}^{k}\ln|\boldsymbol{X}_i| - k\ln|\boldsymbol{X}|\right\}. \quad (3)$$

Setting

$$\begin{aligned} f &= (k-1)p^2 \\ \rho &= 1 - \frac{(2p^2-1)}{6(k-1)p}\left(\frac{k}{n} - \frac{1}{nk}\right) \\ \omega_2 &= \frac{p^2(p^2-1)}{24\rho^2}\left(\frac{k}{n^2} - \frac{1}{(nk)^2}\right) - \frac{p^2(k-1)}{4}\left(1-\frac{1}{\rho}\right)^2 \end{aligned}$$

the probability of finding a smaller value of $-2\rho\ln Q$ is ($z = -2\rho\ln q_{\rm obs}$, where $q_{\rm obs}$ is the observed value of Q)

$$\begin{aligned} P\{-2\rho\ln Q \le z\} \;\simeq\; & P\{\chi^2(f) \le z\} \quad (4) \\ & + \omega_2[P\{\chi^2(f+4) \le z\} - P\{\chi^2(f) \le z\}]. \end{aligned}$$

$P\{-2\rho\ln Q \le -2\rho\ln q_{\rm obs}\} = P\{Q \ge q_{\rm obs}\}$ is the change probability, $1 - P\{-2\rho\ln Q \le -2\rho\ln q_{\rm obs}\} = P\{Q < q_{\rm obs}\}$ is the no-change probability.

2.2. Test for equality of first $j \le k$ complex covariance matrices

If the above test shows that we cannot reject the hypothesis of equality, no change has occurred over the time span covered by the data. If we can reject the hypothesis, change has occurred at some time point. To test whether the first j complex variance-covariance matrices $\mathbf{\Sigma}_i$ are equal, i.e., given that

$$\mathbf{\Sigma}_1 = \mathbf{\Sigma}_2 = \cdots = \mathbf{\Sigma}_{j-1}$$

then the likelihood ratio test statistic R_j for testing the hypothesis

$$H_{0,j} : \mathbf{\Sigma}_j = \mathbf{\Sigma}_1 \;\text{ against }\; H_{1,j} : \mathbf{\Sigma}_j \ne \mathbf{\Sigma}_1$$

is

$$R_j \;=\; \left\{\frac{j^{jp}}{(j-1)^{(j-1)p}}\frac{|\boldsymbol{X}_1 + \cdots + \boldsymbol{X}_{j-1}|^{(j-1)}|\boldsymbol{X}_j|}{|\boldsymbol{X}_1 + \cdots + \boldsymbol{X}_j|^j}\right\}^n$$

or

$$\begin{aligned} \ln R_j \;=\; & n\{p(j\ln j - (j-1)\ln(j-1)) \\ & + (j-1)\ln|\sum_{i=1}^{j-1}\boldsymbol{X}_i| + \ln|\boldsymbol{X}_j| - j\ln|\sum_{i=1}^{j}\boldsymbol{X}_i|\}. \end{aligned}$$

Furthermore, the R_j constitute a factorization of Q

$$Q \;=\; \prod_{j=2}^{k} R_j$$

or $\ln Q = \sum_{j=2}^{k}\ln R_j$. If H_0 is true the R_j are independent. Finally, letting

$$\begin{aligned} f &= p^2 \\ \rho_j &= 1 - \frac{2p^2-1}{6pn}\left(1 + \frac{1}{j(j-1)}\right) \\ \omega_{2j} &= -\frac{p^2}{4}\left(1-\frac{1}{\rho_j}\right)^2 \\ &\quad + \frac{1}{24n^2}p^2(p^2-1)\left(1 + \frac{2j-1}{j^2(j-1)^2}\right)\frac{1}{\rho_j^2} \end{aligned}$$

we get ($z_j = -2\rho_j\ln r_{j,\rm obs}$, where $r_{j,\rm obs}$ is the observed value of R_j)

$$\begin{aligned} P\{-2\rho_j\ln R_j \le z_j\} \;\simeq\; & P\{\chi^2(f) \le z_j\} \\ & + \omega_{2j}[P\{\chi^2(f+4) \le z_j\} - P\{\chi^2(f) \le z_j\}]. \end{aligned}$$

(a) 21 March

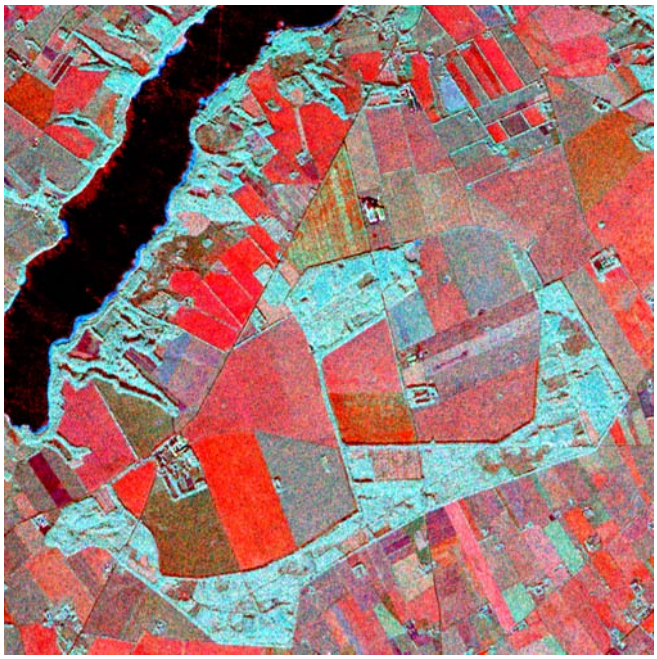

(b) 20 May

Fig. 1. C-band EMISAR data in Pauli representation; same stretching applied to all four images.

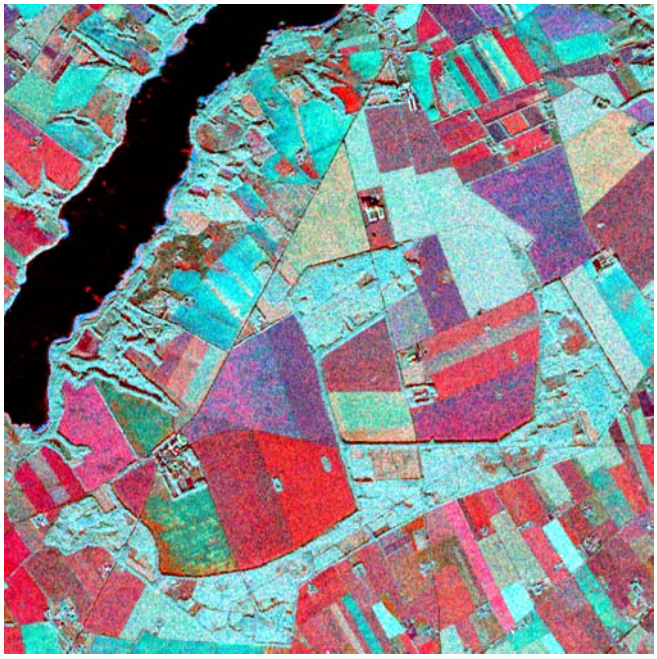

(a) 16 June

(b) 15 July

Fig. 2. C-band EMISAR data in Pauli representation; same stretching applied to all four images.

(a) $-2\rho \ln Q$

(b) p-value

Fig. 3. Test statistic (a) and p-value with grass field marked as black (b); p is approximately 1 in the grass field; in both (a) and (b) dark areas are no-change.

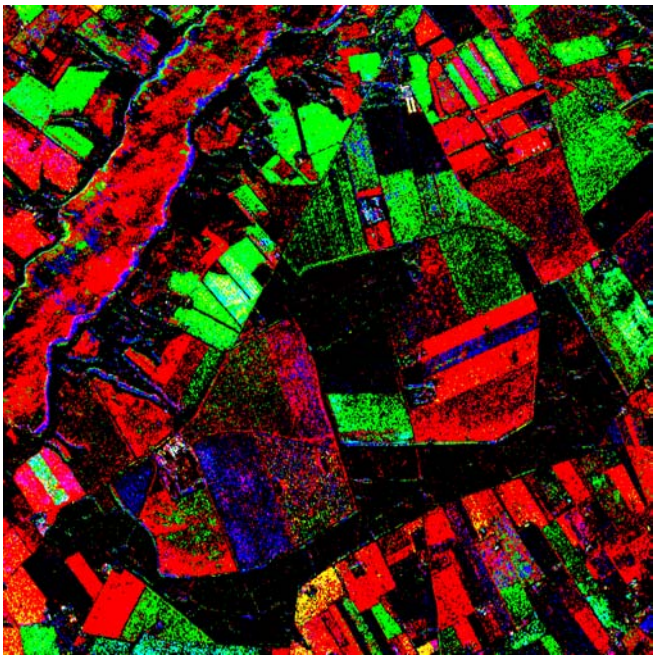

Fig. 4. Shows changes from t_1 to t_2 as blue, from t_2 to t_3 as green, from t_3 to t_4 as red; change probability significance level is 99.99%.

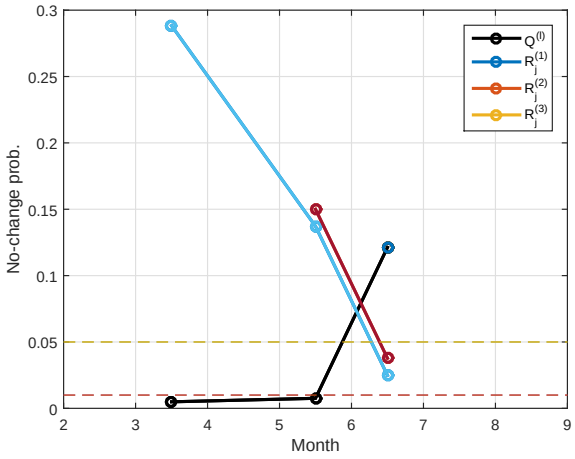

Fig. 5. For the grass field this figure shows average omnibus test based no-change probabilities tabulated in Table 2.

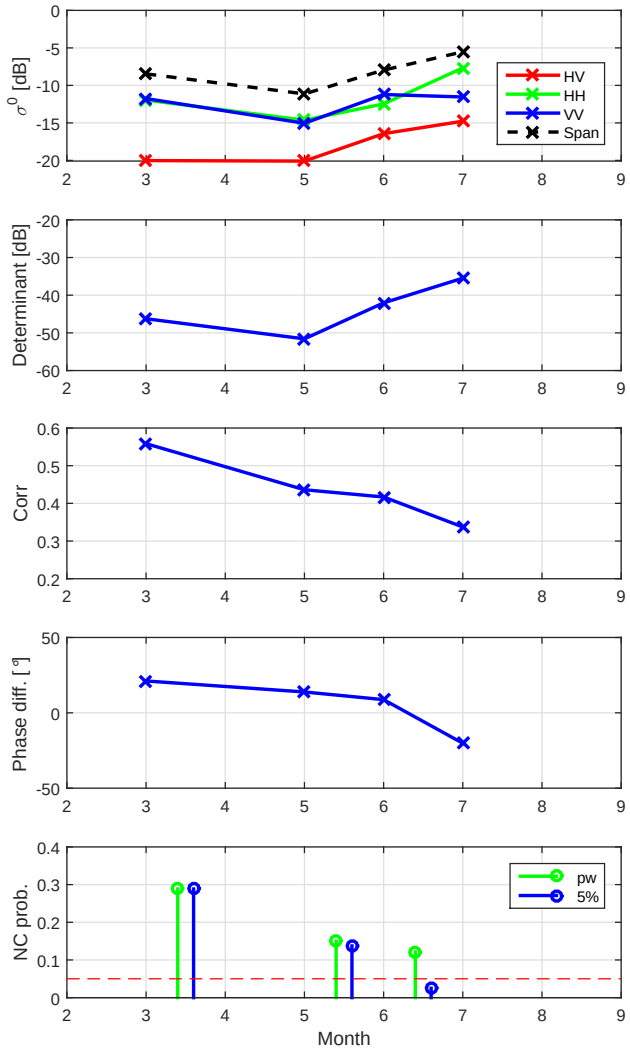

Fig. 6. For the grass field this figure shows average (first plot) backscatter coefficients and span, (second plot) determinant of the covariance matrix, (third plot) magnitude of the correlation between HH and VV, (fourth plot) phase difference between HH and VV, and (fifth plot) pairwise (green stems) and omnibus test based no-change probabilities (blue stems), 5% significance level shown also.

3. CHANGE VISUALIZATION EXAMPLES

To illustrate the above we use full polarimetry EMISAR [6,7] C-band data acquired in 1998 over a Danish agricultural test site on 21 March (t_1), 20 May (t_2), 16 June (t_3) and 15 July (t_4). Figures 1 and 2 show the diagonal elements of the covariance matrix in the Pauli representation where red shows single- or odd-bounce scattering, green shows volume scattering, and blue shows double or even-bounce scattering.

Table 1 shows the change structure built (for each pixel) for an example with data from four time points. The first column indicates which tests are performed for the row in question. The second column shows $Q^{(1)}$ and $P\{Q^{(1)} < q_{\text{obs}}\}$ ("Omnibus" row), or $R_j^{(1)}$ and $P\{R_j^{(1)} < r_{j,\text{obs}}\}$, $j = 2,\ldots,4$ for all time points t_1 through t_4. The third column shows $Q^{(2)}$ and $P\{Q^{(2)} < q_{\text{obs}}\}$ ("Omnibus" row), or $R_j^{(2)}$ and $P\{R_j^{(2)} < r_{j,\text{obs}}\}$, $j = 2,3$ for time points t_2 through t_4. The fourth column shows $Q^{(3)}$ and $P\{Q^{(3)} < q_{\text{obs}}\}$ ("Omnibus" row), or $R_j^{(3)}$ and $P\{R_2^{(3)} \leq r_{2,\text{obs}}\}$ for time points t_3 to t_4. Remember, that for a test for $R_j^{(\ell)}$ to be valid, all previous tests for $R_i^{(\ell)}$, $i = 2,\ldots,j-1$ must show equality, see hypothesis $H_{0,j}$ in Section 2.2.

Note, that $R_2^{(\ell)}$ are the (marginal, non-omnibus) pairwise tests for equality.

3.1. Per pixel change visualization

Figure 3 shows the quantity $-2\rho \ln Q$ and the corresponding p-value, i.e., the change probability.

As an example of per pixel change visualization Figure 4 shows changes from t_1 to t_2 as blue, from t_2 to t_3 as green, and from t_3 to t_4 as red. Black areas have not changed.

3.2. Per field change visualization

Table 2 shows the average no-change probabilities for the grass field shown in Figure 3. Figure 5 shows the same probabilities as graphs, one line per column in Table 2.

As an example of visualization of per field change detection Figure 6 shows mean values over the grass field of the backscatter coefficients and the span (first plot), the determinant of the covariance matrix (second plot), the magnitude of the correlation between HH and VV (third plot), and the phase difference between HH and VV for all four acquisitions (fourth plot). The last plot shows the average pairwise and omnibus based no-change probabilities.

These plots are meant to assist the analyst in determining what caused a possible change, for example an increase in

backscatter as opposed to a decrease in phase angle. We expect that plots like these will be even more useful for interpreting change in longer time series covering for example several years where possible annual oscillations will be important and potentially conspicuous.

Both Table 2, Figures 5 and 6 show that the pairwise tests show no change over time for the grass field. The omnibus test shows change ($P\{Q^{(1)} < q^{(1)}_{\mathrm{obs}}\} = 0.0049$) and the change occurs between June and July ($P\{R^{(1)}_4 \leq r^{(1)}_{4,\mathrm{obs}}\} = 0.0248$).

4. SOFTWARE

We plan to publish Matlab code to perform the analysis described. This will include updating of the change analysis with new data and generation of some of the tables and figures shown above. Also Python code will be made available.

5. CONCLUSIONS

The new omnibus test statistic and its factorization with their p-values show if and when change(s) occur in a time series of multilook, polarimetric SAR data. Contrary to consecutive pairwise comparisons the omnibus test statistic in the example given shows change in C-band SAR data between June and July acquisitions for a grass field.

This type of analysis will become increasingly important and interesting as the databases with relevant SAR data collected routinely and globally keep growing.

6. REFERENCES

[1] K. Conradsen, A. A. Nielsen, J. Schou, and H. Skriver, "A test statistic in the complex Wishart distribution and its application to change detection in polarimetric SAR data," *IEEE Transactions on Geoscience and Remote Sensing*, vol. 41, no. 1, pp. 4–19, Jan. 2003, http://www.imm.dtu.dk/pubdb/p.php?1219.

[2] J. Schou, H. Skriver, A. A. Nielsen, and K. Conradsen, "CFAR edge detector for polarimetric SAR images," *IEEE Transactions on Geoscience and Remote Sensing*, vol. 41, no. 1, pp. 20–32, Jan. 2003, http://www.imm.dtu.dk/pubdb/p.php?1224.

[3] M. J. Canty, *Image Analysis, Classification and Change Detection in Remote Sensing,with Algorithms for ENVI/IDL and Python*, Taylor & Francis, CRC Press, third revised edition, 2014.

[4] A. A. Nielsen, K. Conradsen, and H. Skriver, "Change detection in full and dual polarization, single- and multi-frequency SAR data," *IEEE Journal of Selected Topics in Applied Earth Observations and Remote Sensing*, vol. 8, no. 8, pp. 4041–4048, Aug. 2015, http://www.imm.dtu.dk/pubdb/p.php?6827.

[5] K. Conradsen, A. A. Nielsen, and H. Skriver, "Determining the points of change in time series of polarimetric SAR data," *IEEE Transactions on Geoscience and Remote Sensing*, vol. 54, no. 5, pp. 3007–3024, May 2016, http://www.imm.dtu.dk/pubdb/p.php?6825.

[6] S. N. Madsen, E. L. Christensen, N. Skou, and J. Dall, "The Danish SAR system: Design and initial tests," *IEEE Transactions on Geoscience and Remote Sensing*, vol. 29, pp. 417–426, 1991.

[7] E. L. Christensen, N. Skou, J. Dall, K. Woelders, J. H. Jørgensen, J. Granholm, and S. N. Madsen, "EMISAR: An absolutely calibrated polarimetric L- and C-band SAR," *IEEE Transactions on Geoscience and Remote Sensing*, vol. 36, pp. 1852–1865, 1998.

[8] J. J. van Zyl and F. T. Ulaby, "Scattering matrix representation for simple targets," in *Radar Polarimetry for Geoscience Applications*, F. T. Ulaby and C. Elachi, Eds. Artech, Norwood, MA, 1990.

[9] T. W. Anderson, *An Introduction to Multivariate Statistical Analysis*, John Wiley, New York, third edition, 2003.